ABRASION RESISTANT METALLIC ALLOYS FOR THE MINING INDUSTRY

E. Albertin[1] and A. Sinatora[2]

[1]Institute for Technological Research of São Paulo State, Metallurgy Division, São Paulo, Brazil
[2]University of São Paulo, Surface Phenomena Laboratory, Department of Mechanical Engineering, São Paulo, Brazil

Keywords: Abrasion, Abrasion Resistant Materials, Mining, Niobium

Abstract

In the mining industry, abrasion is the most significant wear mechanism. The resistance to abrasion is a property that must be combined with other material properties, such as toughness and corrosion resistance. In the crushing, grinding and material handling operations, the most relevant wear resistant materials are steels and cast iron.

Pearlitic and martensitic steels compete in applications, such as lifters and liners for SAG mills. Martensitic steel can also be the material choice for large balls for SAG mills, chutes and wear plates for heavy trucks. Austenitic manganese steel remains the proper choice for jaws or cone crushers. In applications with lower impact demands, high chromium cast irons are widely used for balls and liners. All these materials are subjected to increasingly higher stresses as the size of all such equipment is increasing over time.

The wear performance of such steels has been improved by refining the pearlite, increasing the hardness of martensite and increasing the work hardening of austenite. In cast iron, the approach has been to optimize the matrix hardness and adjust the carbide content according to the application.

Niobium has been investigated in the improvement of wear resistance due to its multiple effects; Niobium can harden pearlite due to grain refinement, it can harden the martensite due to precipitation hardening and can form very hard NbC carbides from the melt.

This paper critically reviews the literature with regard to improvement of the abrasive wear resistance of pearlitic, martensitic and austenitic steels, and high chromium cast irons. This paper also presents test results obtained from different materials containing niobium, with the aim of ranking them for applications where abrasion is the predominant wear mechanism.

Introduction

Abrasion in the mining industry is the wear mode that reduces the thickness, diameter and height of components used to crush, grind, sieve, store and transport mineral goods. The main consequences of abrasion are safety and environmental risks, as well as decreasing efficiency, increasing energy losses, increasing the maintenance time, and thus losses in production and productivity.

Engineers look for simple abrasion models to predict thickness, diameter, height, mass, noise or any other variable that would allow them to know within a certain margin of uncertainty when to replace the parts subject to abrasion. A graphical description that relates abrasion models and life of wear parts is presented in Figure 1.

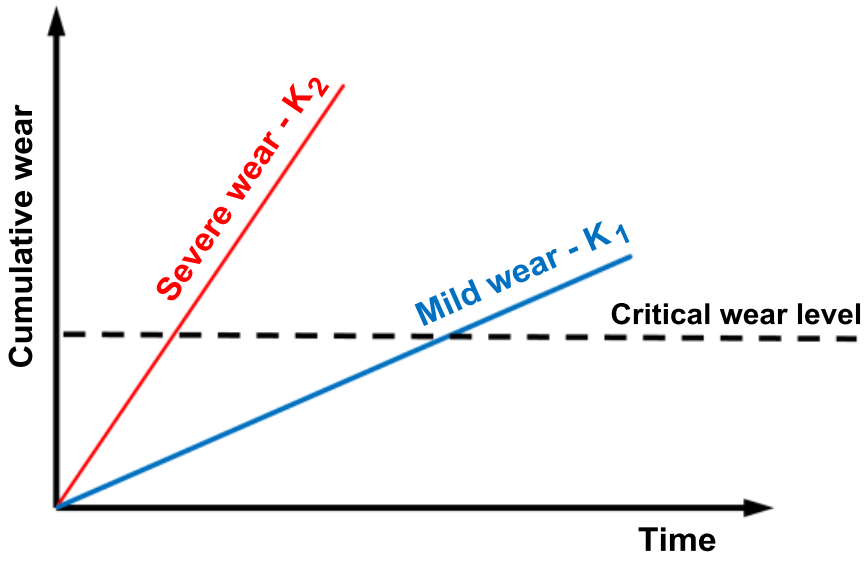

Figure 1. Cumulative wear vs time. When the cumulative wear intercepts the critical wear level the wear part needs to be replaced. Holmberg [1].

In Figure 1, both the severe and mild wear cases were drawn as straight lines, which is the case in a large number of abrasion phenomena. K is the gradient of the straight lines in Figure 1 and therefore, it expresses the intensity of abrasion, being greater for the severe wear case (K_2) than for the mild wear case (K_1). The well-known abrasion model proposed by Rabinowicz tries to estimate the mass loss based on applied load, material hardness and abrasive particle geometry, as in Equation 1 [2].

$$Q = k_i \frac{W}{H} \tag{1}$$

where:
Q is the cumulative mass loss (kg),
W is the normal force (applied load) (N),
H is the abrasion resistant material hardness (Pa), and
k is a constant related to the abrasive geometry (kg/m^2).

The first outcome from Figure 1 and Equation 1 is that there are simple (linear) and useful predictive models to be used in maintenance planning to estimate the replacement time for components. Graphs for mild and severe wear conditions can be easily obtained in the laboratory. The challenge of how to link laboratory studies and service performance in order to predict component life will be scrutinized in a later paper in this conference [3].

A second consequence is that, in order to increase service life of an abrasion resistant component, represented by the elapsed time until the straight line intercepts the critical wear level, it is necessary to "push" the constant K from K_2 to K_1. The terms "severe" and "mild", from Figure 1, are more properly defined in connection with the abrasion mode of wear in Table I, from Gates [4]; it is possible to associate the constant K to some variables of the tribosystem.

Table I. Proposed Severity-based Classification for Abrasive Wear [4]

Typical Situations	**Abrasive Wear Mode**		
	Mild	**Severe**	**Extreme**
Particle size	Small	Moderate	Large
Constraint	Unconstrained	Partially constrained by counterface	Strongly constrained
Particle shape	Rounded	Sharp	Sharp
Contact stress	Low – insufficient to fracture particles	Moderate – sufficient to fracture particles	Very high – may cause macroscopic deformation or brittle fracture of material being worn
Dominant mechanisms	Microplowing	Microcutting	Microcutting and/or microfracture
Equivalent terms	● Low-stress abrasion	● High-stress abrasion	● Gouging abrasion
	● Scratching abrasion	● Grinding abrasion	
	● Low-stress three-body	● High-stress three-body	● High-stress two-body
		● Low-stress two-body	

Increasing abrasive particle size, abrasive sharpness and the external load lead to microcutting abrasion micromechanism, promoting, therefore, the severe abrasion regime (K_2). Increasing the abrasive hardness will also act to promote the severe abrasion mode. Small abrasive grains, rounded grains and low loads, promote the micromechanism of microplowing and, therefore, the mild abrasion regime (K_1).

An increase in the material hardness will contribute to reducing the constant K. However, it is well known that the behavior of an abrasion resistant material does not depend solely on its own hardness but also on the hardness of the abrasive media. This concept is expressed in Figure 2, from Zum Gahr [5].

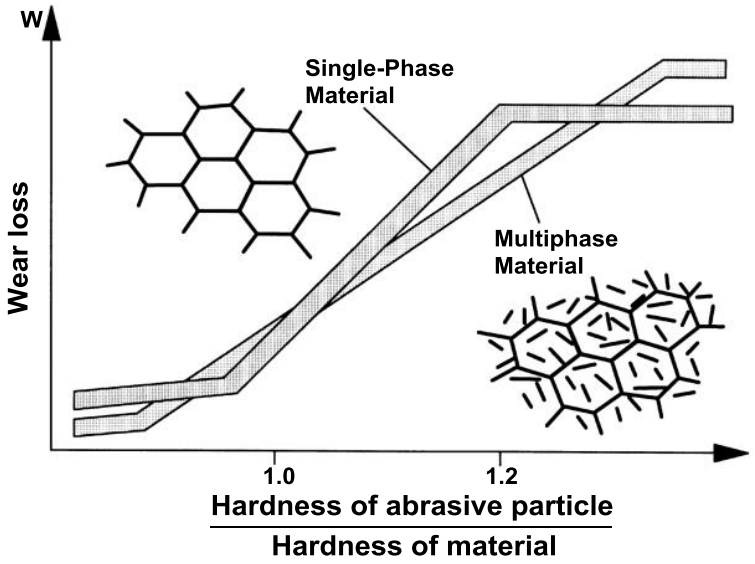

Figure 2. Schematic representation of wear regimes as a function of the relationship between the hardness of abrasive particles and the hardness of the abrasion resistant material. Adapted from Zum Gahr [5].

The Effect of Hardness on Abrasion

To investigate the mild and severe abrasion regimes, several steels and cast irons were studied in laboratory, pin on disc, abrasion tests. Table II summarizes the most relevant data for the materials. Figures 3(a), (b) and (c) are representative microstructures of the cast irons tested and Figures 4(a) and (b) present the wear and friction data.

Table II. Summary of Heat Treatments and Microstructures of the Tested Materials. Pintaúde, et al [6]

Material	Heat Treatment	Expected Microstructure
52100 steel	Oil-quenched after holding at 900 °C for 60 min, tempering at 500 °C for 24 h	Tempered martensite + M_3C carbides
1070 steel	Water-quenched after holding at 860 °C for 60 min, tempering at 250 °C for 50 min.	Tempered martensite
Ductile iron	Oil-quenched after holding at 860 °C for 60 min, double tempering at 370 °C for 90 min plus 60 min, and sub-zero treatment, maintaining in liquid nitrogen for 120 min.	Tempered martensite + graphite nodules
White cast iron	Annealing at 700 °C for 8 h. Air-quenched after holding at 1000 °C for 40 min.	Martensite + M_7C_3 carbides
Multicomponent	Double tempering at 550 °C for 180 min. Air-quenched after holding at 1000 °C for 40 min. Double tempering at 600 °C for 240 min plus 180 min	Tempered martensite + (MC + M_2C) carbides + secondary precipitates

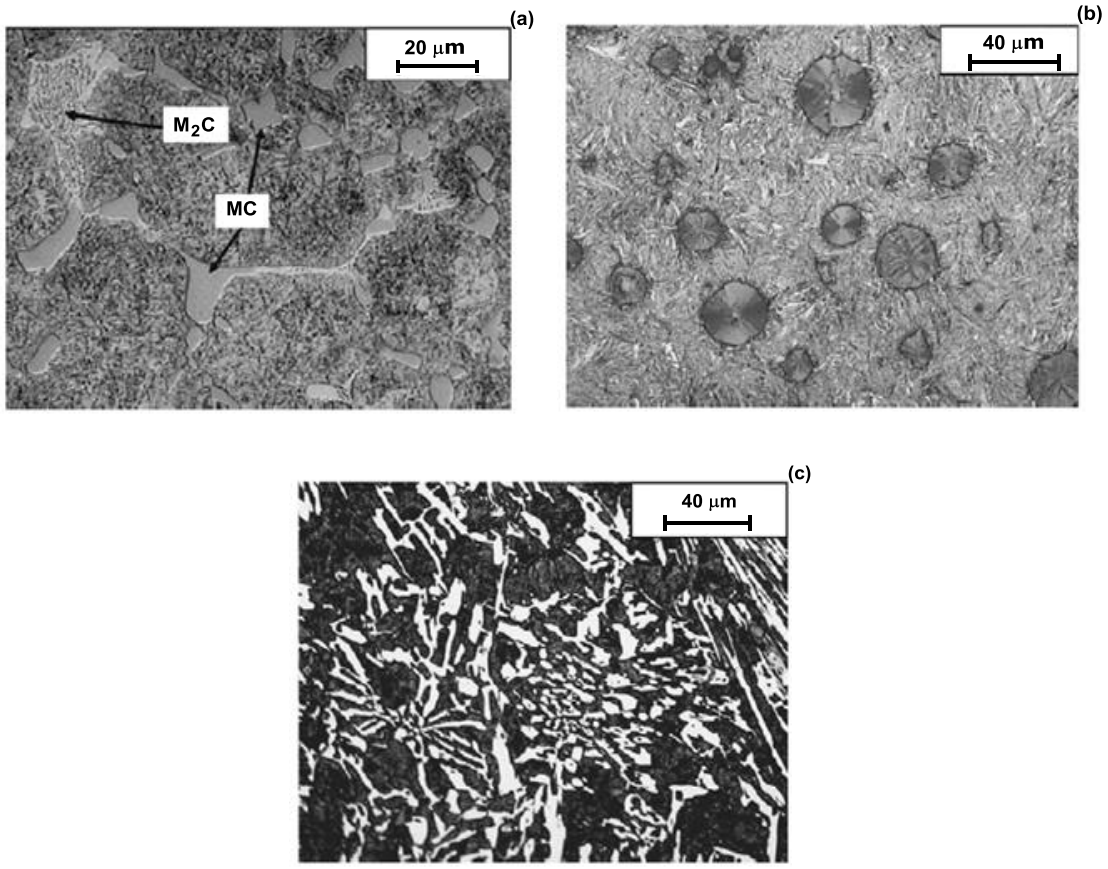

Figure 3. Microstructure of tested cast irons; (a) multicomponent cast iron, martensite + MC and M_2C carbides, (b) ductile cast iron, martensite + graphite nodules and (c) high-chromium cast iron, martensite + M_7C_3 carbides. Pintaúde, et al [6].

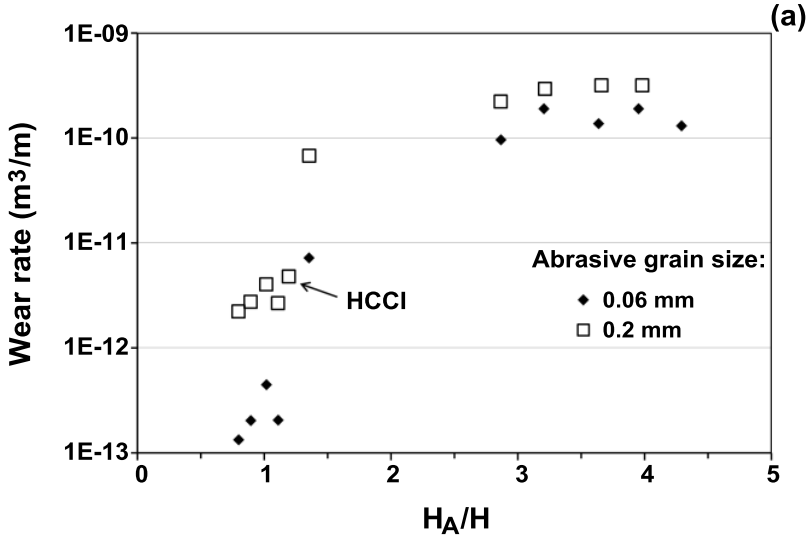

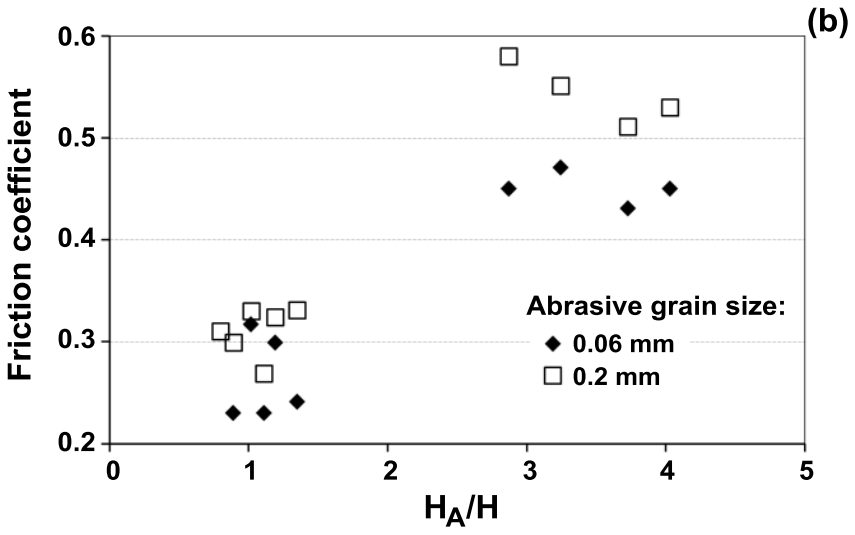

Figure 4. (a) Relationship between wear rate (m^3/m) and the ratio of the abrasive hardness (H_A) and material bulk hardness (H) and (b) friction data. Single phase materials. Pintaúde et al. [6]. (HCCI: high Cr cast iron.)

The wear rate increased by approximately three orders of magnitude with increasing H_A/H. The abrasive grain size played a more significant part in the tests where the lower abrasion rates were measured. Two levels of friction coefficient were observed: from 0.2 to 0.3 and from 0.4 to 0.6, approximately. Lower wear rates and lower friction coefficients were associated with smaller abrasive grain sizes and with the prevalence of microplowing instead of microcutting.

To reduce the wear rates, the H_A/H ratio must be decreased. Most of the time the abrasive hardness cannot be chosen since it depends on the mineral being mined. Therefore, the increase in the material hardness is the main factor to be engineered in Figure 4, to reduce abrasion.

The hardness of single-phase material with martensitic matrices is limited to the tempered hardness of martensite and the compromise between hardness and toughness necessary for optimum behavior in service. Therefore, a series of high chromium cast irons (HCCI) with M_7C_3 carbides and with austenitic and martensitic matrices, as well as cast high speed steels (MCI), quenched and tempered, were investigated with a pin on disc experimental set-up. The wear rate and the friction data are presented in Figure 5 [7]. Composition data for these alloys are depicted in Table III.

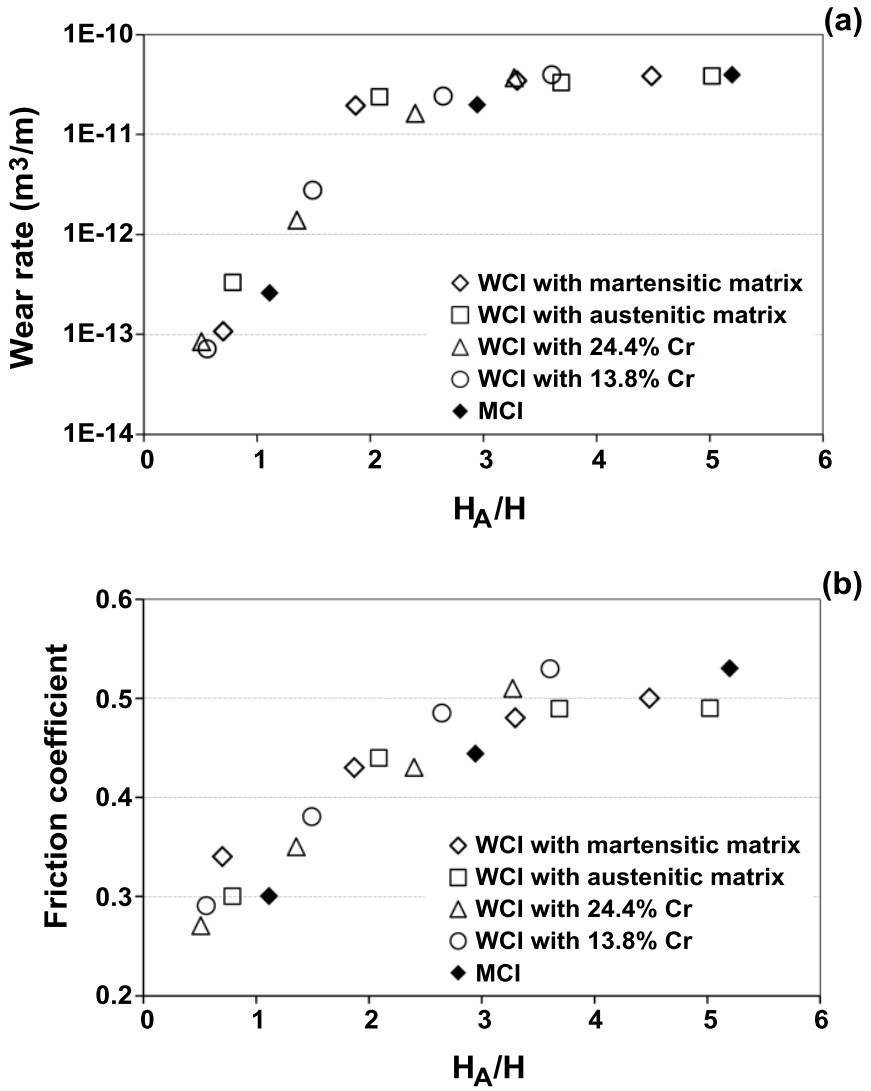

Figure 5. (a) Relationship between wear rate (m^3/m) and the ratio of the abrasive hardness (H_A) and material bulk hardness (H) and (b) friction data. Hard second-phase materials. Coronado et al. [7].

Table III. Composition (%wt.) of the Hard Second Phase Materials. Coronado et al. [7]

Material	Cr	C	Si	Mn	S	Mo	Ni	Nb + Ti
WCI 13.81 wt.%Cr	13.81	5.06	0.27	0.42	0.005	-	-	-
WCI 24.41 wt.%Cr	24.41	3.14	0.36	0.36	0.013	-	-	-
MCI	1.4 – 2.1	3 – 3.6	0.5 – 1.25	0.45 – 1.3	0.005	0.25 – 0.7	4.1 – 4.8	3

The wear rates varied by approximately three orders of magnitude, as already shown in Figure 4 for single phase materials. The friction coefficient increased steadily from 0.2 to 0.6, approximately. As in the previous series of tests, the lower wear rates and lower friction coefficients were associated with the prevalence of microplowing instead of microcutting.

The wear regions, predicted in Figure 2, are experimentally revealed in Figures 4(a) and 5(a), as well as the transition between the two wear regimes. For the materials with large and hard second phases, Figure 5(a), the severe wear region has lower wear rates than materials without large hard second phases, as also predicted in Figure 2.

There are also some differences between Figures 2 and 4. The end of the severe region and the beginning of the transition to the mild one occurs in Figure 2 at a value of H_A/H of 1.2. This is based on the predictions of Torrance [8], where the indentation stresses of a perfectly rounded particle were used to calculate the minimum hardness differences (20% in this case) necessary for a hard body to penetrate a soft one. A second condition, assumed in Figure 2, is that the materials have elasto-plastic behavior; that means they do not work harden as they are worn out, or in other words, that during the wear process they keep their original bulk hardness. The abrasives in the tests in Figure 4 were sharp instead of rounded and work hardening occurred as will be seen later. Therefore, the transition regions on the experimental curves are displaced to greater values of H_A/H, in comparison with the Zum Gahr model.

Both Figures 4(a) and 4(b) show that the reduction in the abrasion with reduced H_A/H is less pronounced in the severe wear region, that is, a great increase in material hardness is necessary to result in a small reduction in the abrasion rate. On the contrary, if the wear occurs in the transition region, a small increase in the hardness of the abrasion resistant material results in a large decrease in the wear.

These conclusions are of importance in the evaluation of results of laboratory wear tests. An analysis of the real tribosystem is, therefore, necessary in order to adjust the severity of the laboratory tests to the field conditions. If the field tribosystem promotes abrasion in the mild regime or in the transition region, the laboratory test cannot be performed with hard abrasives (tests in the upper plateau of the graphs). With such a test configuration, the abrasion resistance increase might be considered unimportant or uneconomical, since with this test condition, with high wear rates, the effect of increasing the abrasive's hardness is intrinsically small.

Figures 4(a) and 5(a) allow us to predict that for abrasion in the severe regime, the increase in abrasion resistance attainable with the addition of a hard second phase will be as large as one order of magnitude (from $k = 10^{-10}$ m^3/m in Figure 4(a) to $k = 10^{-11}$ m^3/m in Figure 5(a) for a constant material hardness. As a consequence, to further improve wear resistance, it will be necessary to add second hard phases and to increase the bulk hardness to reach the transition region of the graphs. The increase of the bulk hardness for wear plate material, steels and weld deposits, Figure 6, was studied in dry rubber wheel testing (RWAT).

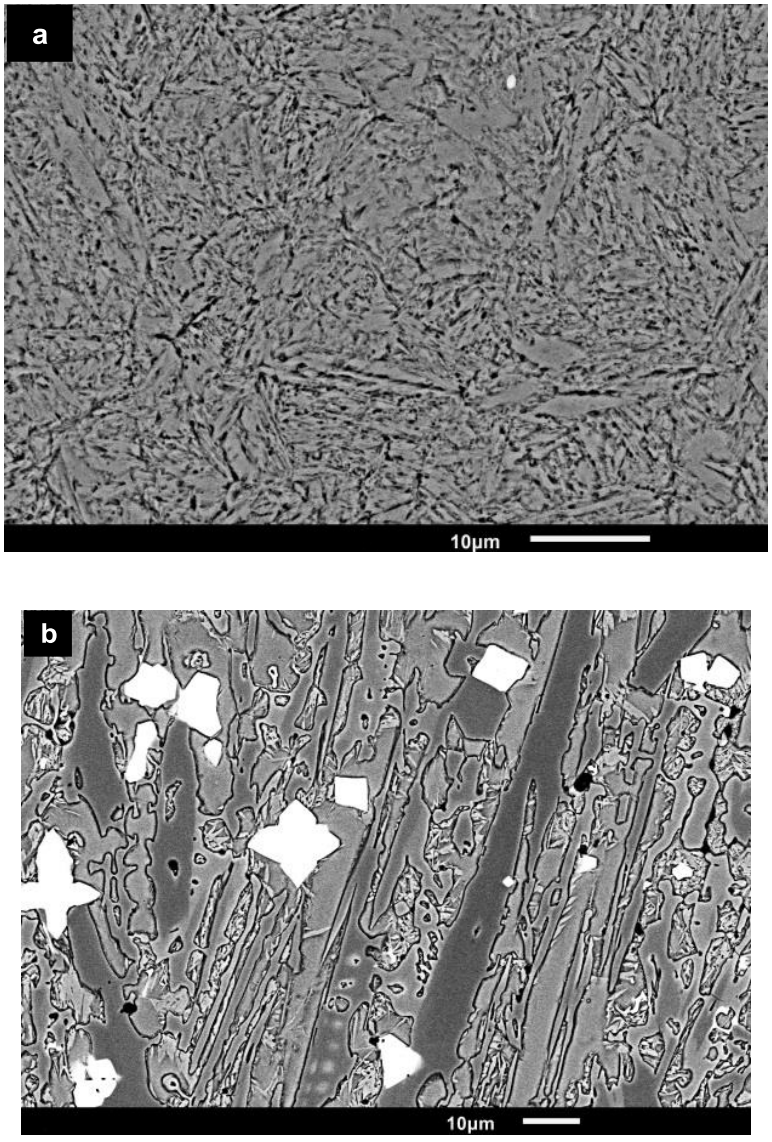

Figure 6. (a) Martensitic Q & T steel, (b) Weld deposit. M_7C_3 carbides, NbC carbides in an austenitic matrix.

As expected, the increase in hardness reduced the wear coefficient for both sets of materials. It is apparent that the gradient of the abrasion data for steel, K_2, is greater than for the weld deposits K_1. The RWAT abrasion tests were performed with silica sand (1000 to 1200 HV), H_A/H in the range of ~8.7 to 1.5 and the effect of the relative hardness is shown in Figure 7(b).

This figure shows that possibly there is a mild to severe wear transition similar to those shown in Figures 2, 4 and 5 for three-body abrasion tests. There remains a question: how to compare two-body and three-body wear rates or wear coefficients?

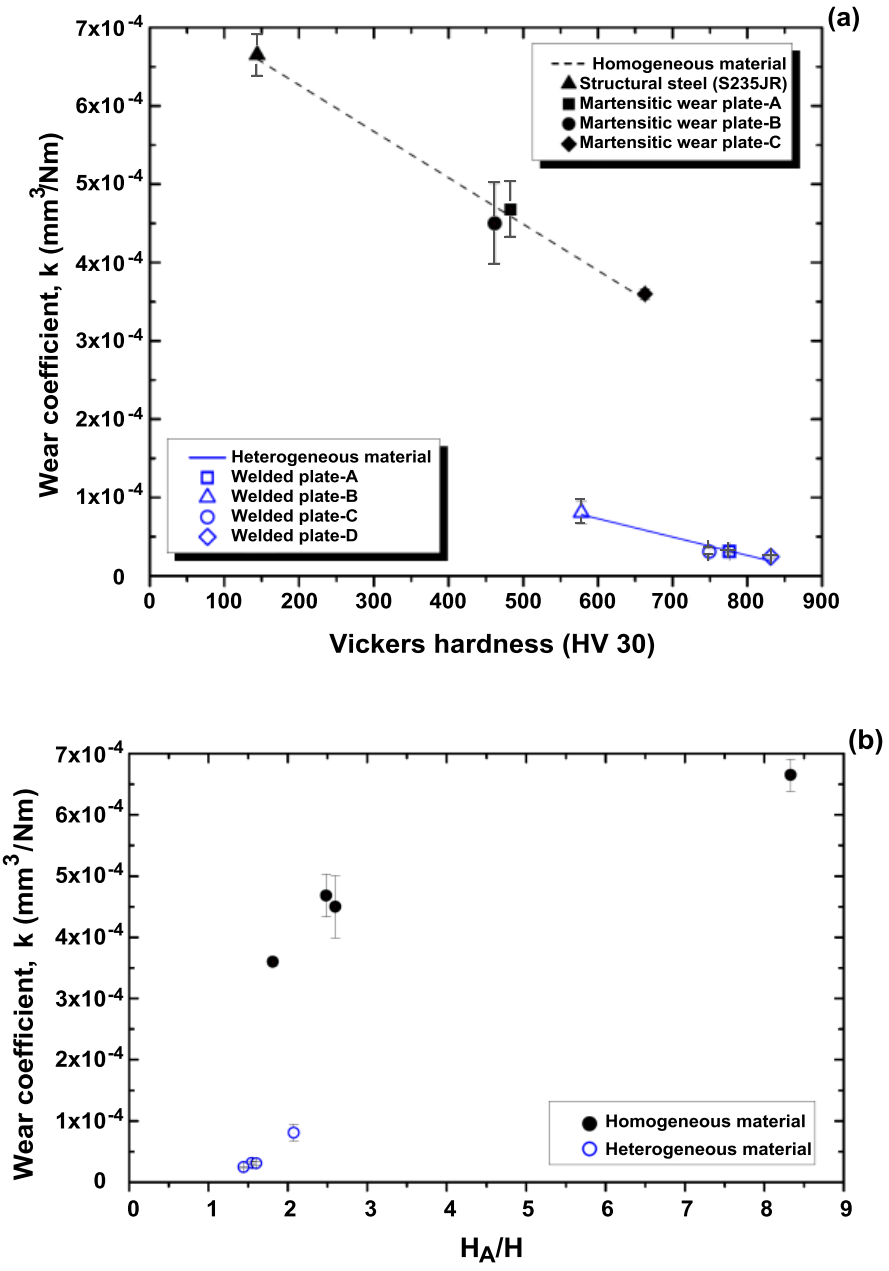

Figure 7. Wear coefficient for materials without big hard second phase, dashed line, and for materials with big hard second phase, solid line. RWAT, silica sand # 100, 130N; (a) Wear x Hv, (b) Wear x H_A/H. Penagos, Tressia and Sinatora [9].

It is also remarkable in Figure 7(a) that a hypothetical single phase material with a hardness of 600 HV would have a wear coefficient of approximately 4.0 x 10^{-4} mm^3/Nm and the addition of a second hard phase would increase its wear resistance, bringing the wear coefficient to 0.8 x 10^{-4} mm^3/Nm, a fivefold decrease. However, if, simultaneously to the addition of the second hard phase, the bulk hardness had been increased to 830 HV, the abrasion coefficient would be reduced to 0.25 x 10^{-4} mm^3/Nm, one order of magnitude increase of the abrasion resistance. The same

tendency for cast materials with hard second phases is observed in Figure 8. Those trends were already observed in Figures 2 and 4.

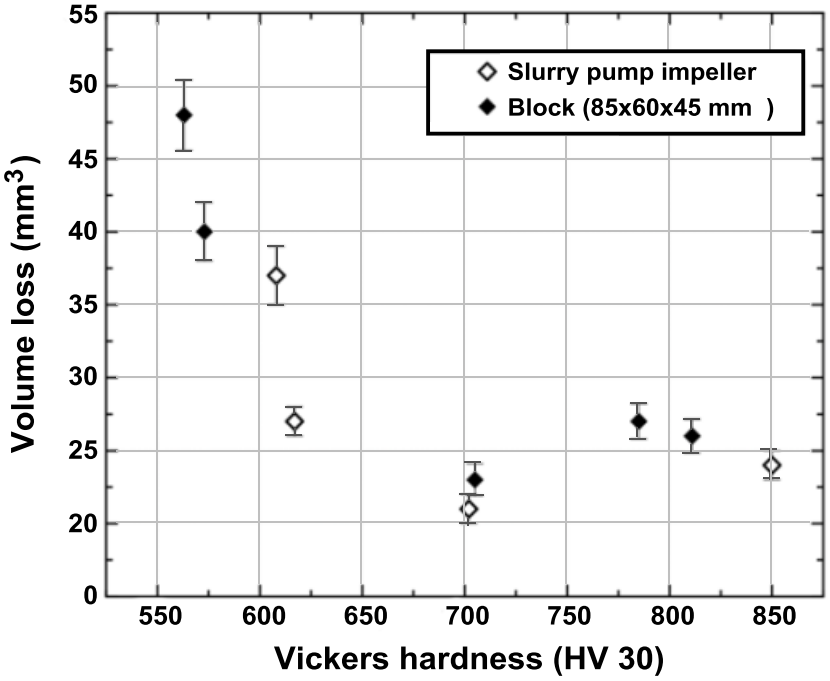

Figure 8. Volume loss for cast materials with large hard second phase, RWAT, silica sand # 50, 130 N. Penagos and Sinatora [10].

After considering the approach to reduce abrasion based on hardness, let us consider some effects not directly connected to hardness.

The Effect of Other Parameters on Abrasion

Microstructure

In order to study the effect of microstructure refinement, white cast iron alloy blocks were cast in a sand mold with a chill plate, as shown in Figure 9. Alloys with 0.6%Nb had their abrasion resistance compared, after quenching and tempering procedures, in a pin on disc and in the dry RWAT test [11].

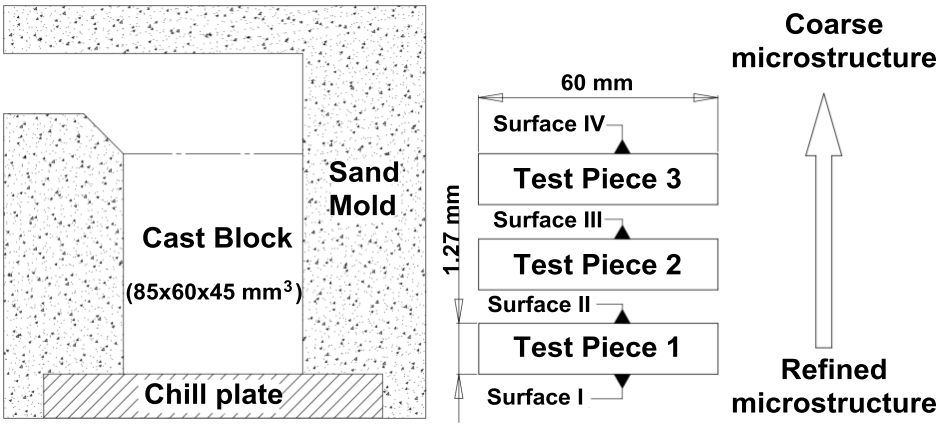

Figure 9. Experimental set-up to change carbide spacing (mean free path) of 2.8%C, 18.8%Cr and 0.6%Nb white cast iron.

The casting plus heat treatment procedure resulted in a peculiar match of carbide spacing and hardness. Figure 10 shows that there was a pronounced grain refinement, and quantitative metallography showed that at the two surfaces closer to the chill plate, the carbide spacing decreased significantly. The two other surfaces had similar austenitic grain size and carbide spacing. As the carbide spacing increased, the width of the carbides also increased. The bulk and microhardness, however, were quite similar for the three samples nearer the chill plate, as shown in Table IV.

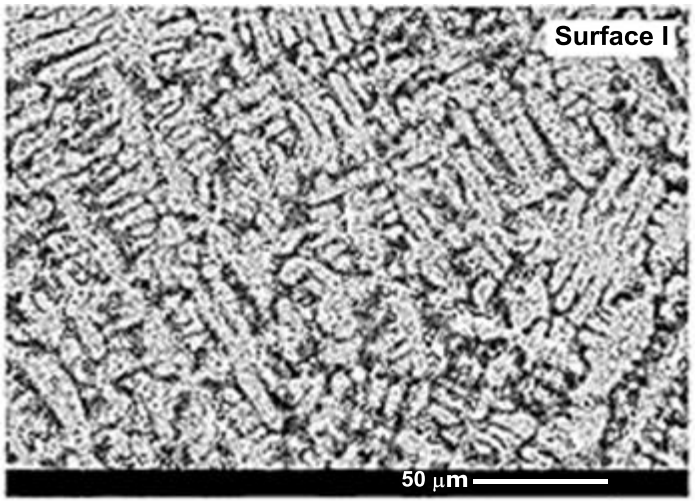

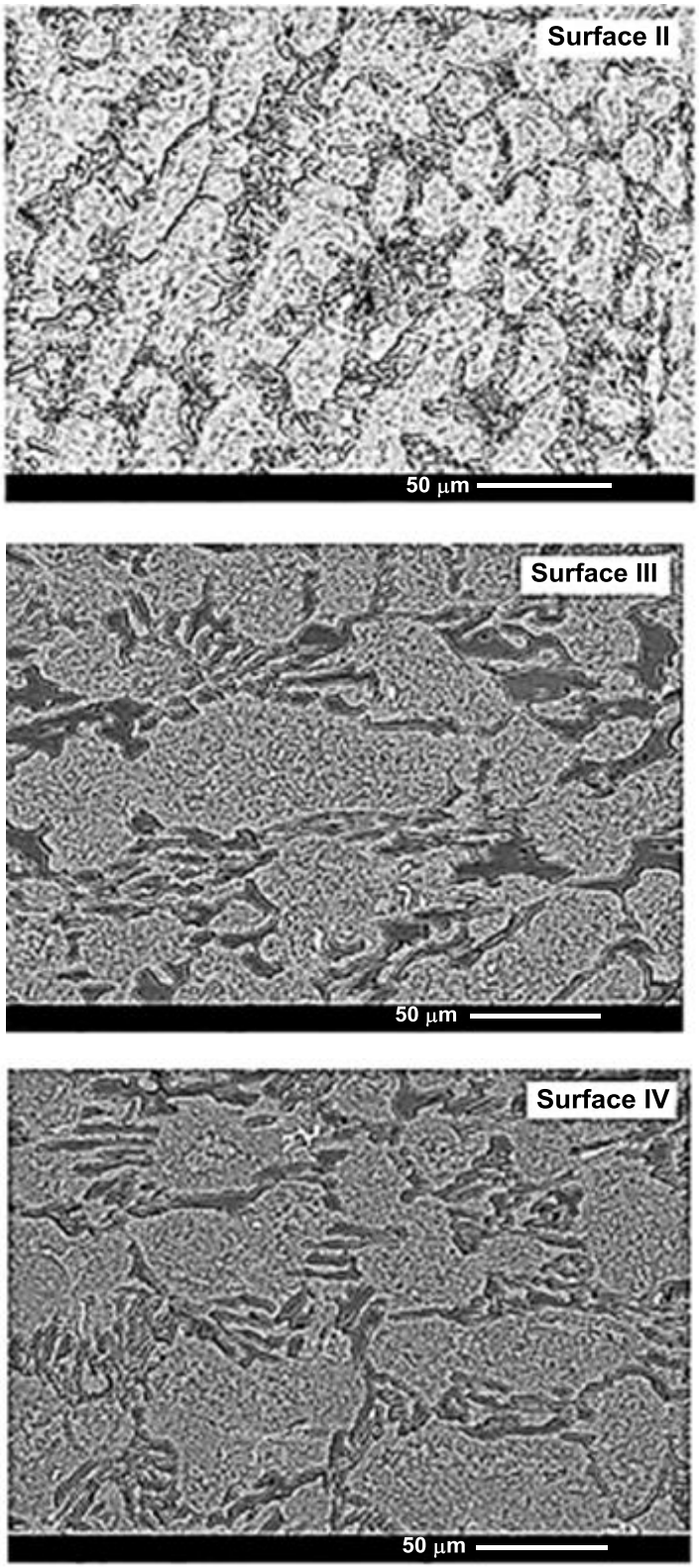

Figure 10. Micrographs of the 2.8%C, 18.8%Cr. Martensite + eutectic of martensite + M_7C_3 carbide.

Table IV. Hardness of Materials and Phases

Test Surface	Material Macrohardness HV 30	Matrix Microhardness HV 0.1	M_7C_3 Hardness HV 0.25
I	806 ± 3	760 ± 19	-
II	811 ± 8	752 ± 43	-
III	802 ± 4	728 ± 9	1473 ± 253
IV	784 ± 8	708 ± 12	1437 ± 300

As a consequence of the increase in carbide spacing and in carbide coarsening, there was an abrasion reduction of more than 30% for both pin on disc and dry RWAT tests when the two slices near the surface were compared (Figure 11).

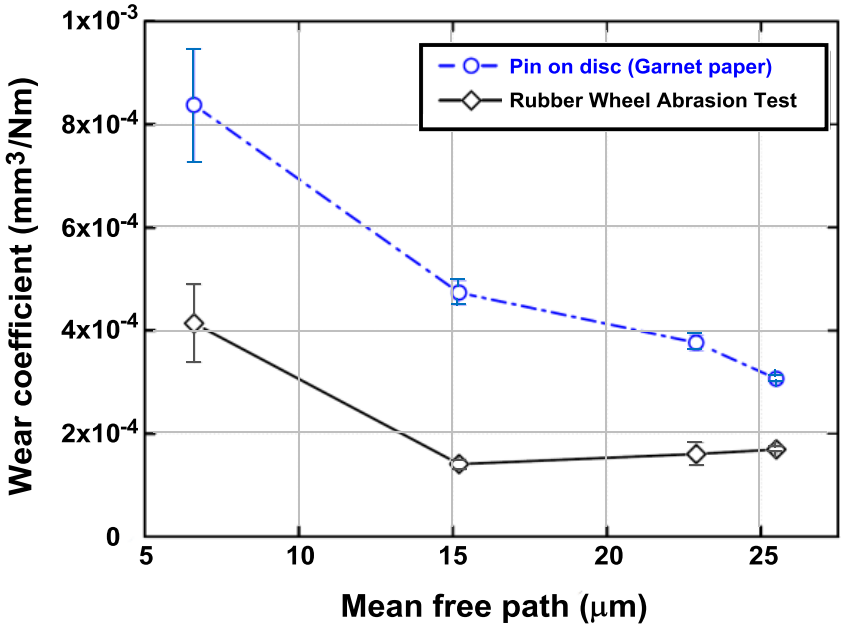

Figure 11. Wear coefficient as a function of carbide spacing. Pin on disk abrasive garnet. Dry RWAT, silica 2.8%C, 18.8%Cr, and 0.6%Nb alloy.

This result is probably due to the more effective barrier exerted by the thicker carbides as is to be seen in Figure 12. The thicker carbides were able to resist cracking and therefore, were able to restrain the width of the abrasion marks when compared with samples with thinner and less spaced carbides.

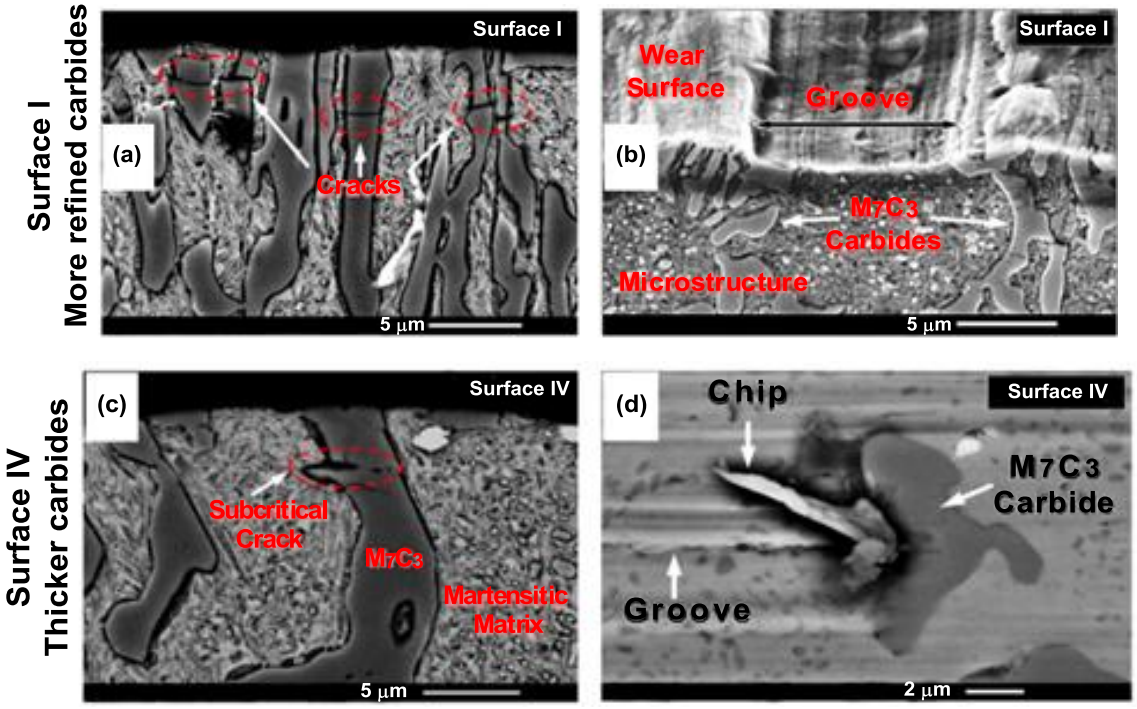

Figure 12. (a) Subsurface microstructure of thinner carbides for the more refined structure, (b) subsurface microstructure and taper section for the more refined structure (surface I), (c) subsurface microstructure and (d) wear surface for thicker carbides. Note that thicker carbides are less susceptible to cracking and fracture and can occasionally act as a barrier to abrasive grit, resulting in a higher wear resistance. Penagos et al [11].

The comparison of abrasion results for the base alloy and the alloy with 0.6%Nb from dry RWAT tests is shown in Figure 13. No significant hardness change was measured for equivalent samples. Besides that, it is noticeable that the carbide coarsening reduced the abrasion, a promising effect of niobium that is under investigation.

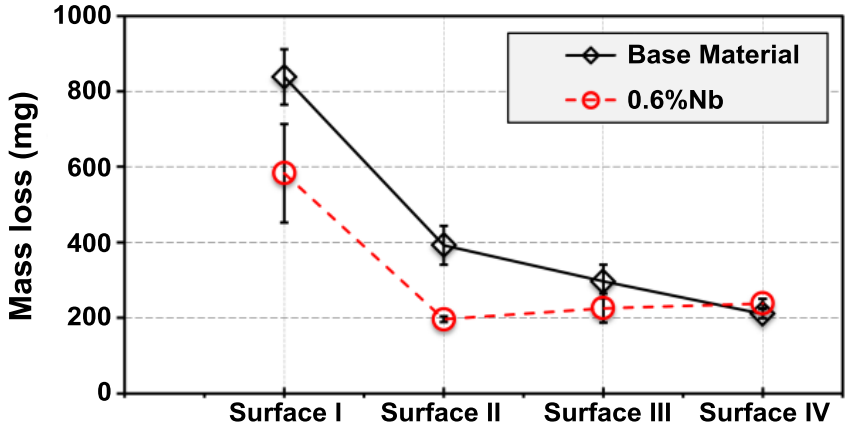

Figure 13. Mass loss, dry RWAT, 130 N, # 100, 2.8%C, and 18.8%Cr, without and with 0.6%Nb alloy.

Another example where the microstructural parameters prevailed over the hardness effect was detected in a series of high carbon, high speed steels containing niobium (compositions presented in Table V). For these alloys, the carbon content was adjusted, providing extra carbon as the niobium content was increased, in order to keep the same carbon content in the matrix [12].

Table V. Chemical Composition of the HSS-Nb Alloys

Alloys	**Chemical Composition (wt.%)**						
	C	**Cr**	**Mo**	**W**	**V**	**Nb**	**Ti**
Nb0	0.51	4.18	3.27	1.91	0.97	-	-
Nb2.5	0.81	3.94	3.32	2.33	0.92	2.52	-
Nb2.5Ti	0.81	3.94	3.09	2.23	0.91	2.81	0.11
Nb5	1.05	3.81	3.33	2.83	0.92	5.73	-
Nb5Ti	1.07	3.80	3.07	2.56	0.92	5.73	0.09

All cast samples were annealed (700 ºC, 5 h, furnace cooling). The entire test pieces were heat treated through quenching (austenitization at 1100 ºC, 2 h, still air cooling) and double tempering (500 ºC, 2 h, still air cooling). For all the alloys, resultant bulk hardness ranged from 680 to 740 HV 30, while matrix microhardness ranged from 630 to 700 HV 0.1. The relevant microstructures are shown in Figure 14.

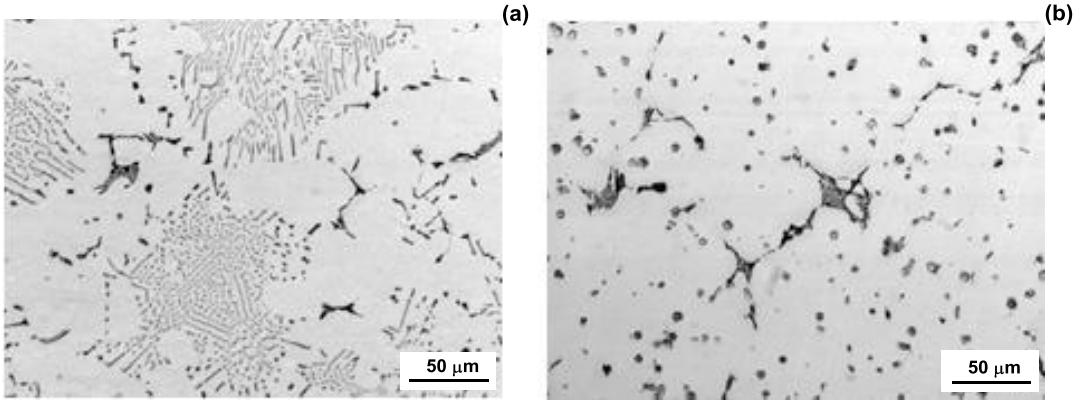

Figure 14. Distribution and morphological details of the eutectic carbides in the microstructure of the HSS-Nb alloys Nb2.5 (a), and Nb2.5Ti (b) [12].

The alloy without Nb (Nb0) was cast with the same matrix composition as the other four alloys, but without carbides. The effect of the hard carbides is apparent since the Nb0 alloy showed the highest wear coefficient, evaluated through dry RWAT using hematite as the abrasive, Figure 15. Examination after the test revealed that the carbides of the alloys Nb5 and Nb5Ti suffered cracking resulting in higher wear coefficients than for Nb2.5 alloys.

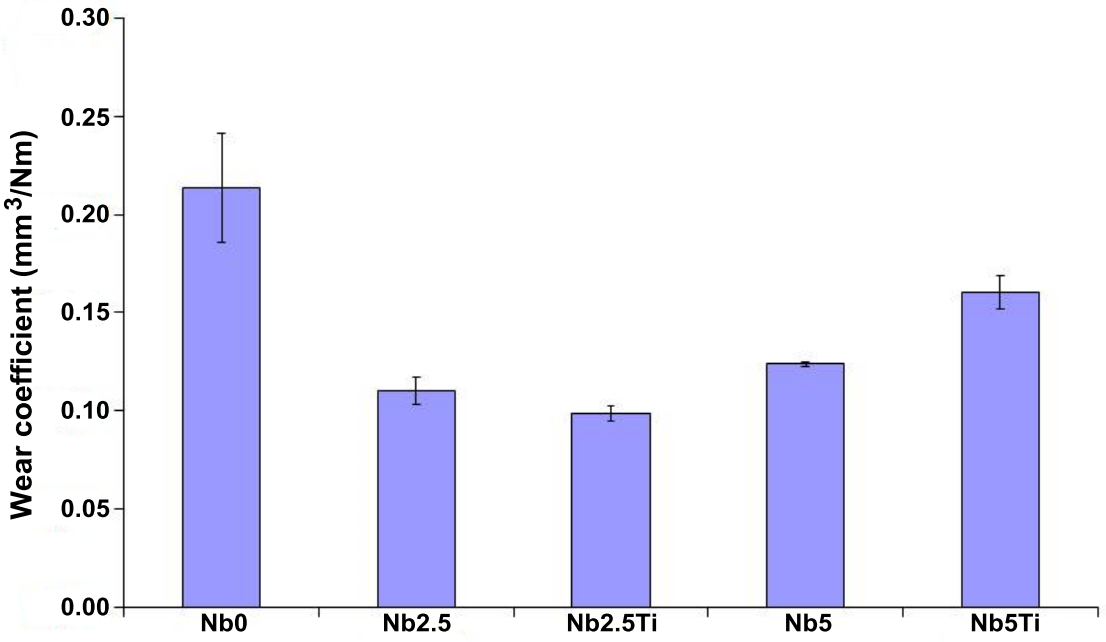

Figure 15. Wear coefficient of the HSS-Nb alloys. RWAT: 130 N, 200 rpm, 30 min, hematite (-210 μm+105 μm; 860 HV 0.1) [12].

The Nb2.5 alloy showed Chinese script-like eutectic NbC carbides in the form of eutectic cells, while the Nb2.5Ti alloy contained polygonal divorced NbC carbides. Microstructural examination after the wear test showed that for the abrasion tests performed with hematite, just part of the Chinese script carbide was pulled out along with the matrix in the Nb2.5 alloy. Moreover, the polygonal divorced carbides of the Nb2.5Ti alloy were not pulled out, even when the matrix was severely worn, as shown in Figure 16.

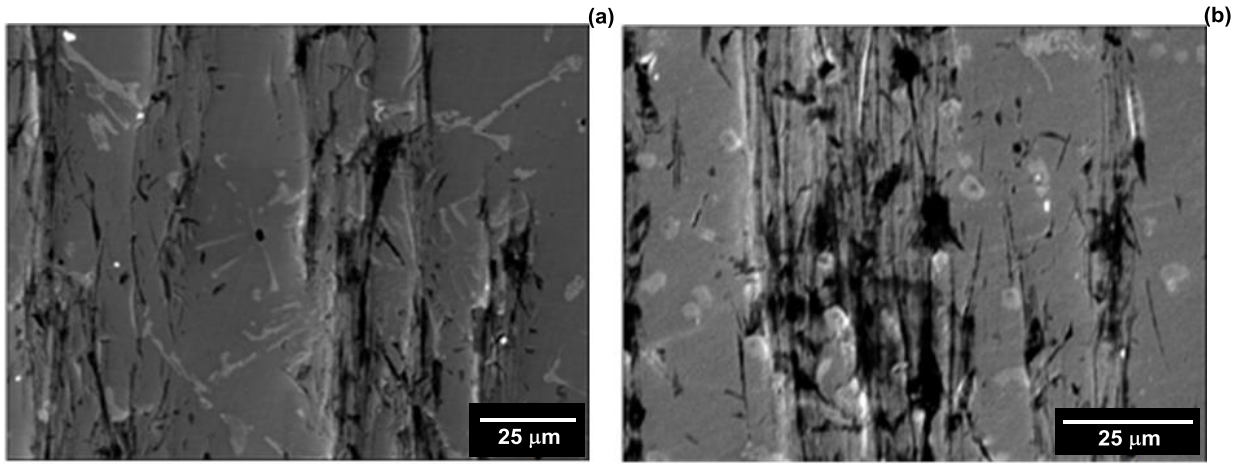

Figure 16. Details of the worn test piece of the Nb2.5 alloy (a) and the Nb2.5Ti alloy (b). SEM – back-scattered electrons [12].

A microstructural analysis was attempted to rationalize the abrasion behavior of those alloys, noting a clear relationship with carbide perimeter, as shown in Figure 17. Further investigation might confirm a linear correlation between carbide perimeter and wear coefficient, as well as indicate whether the result for Nb2.5Ti alloy is actually a minimum.

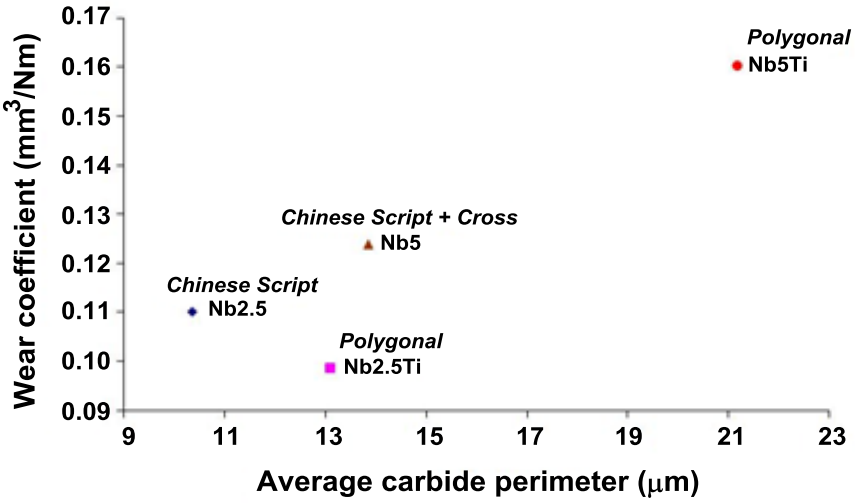

Figure 17. Relationship between wear coefficient and average NbC carbide perimeter [12].

Carbon Content

Apart from the microstructure, some results also show a correlation between the carbon content of the alloys and their abrasion resistance. Figure 18 presents data from ongoing research on the abrasion resistance of 13% manganese steel (Hadfield) with similar bulk hardness, used in crushing operations at mines.

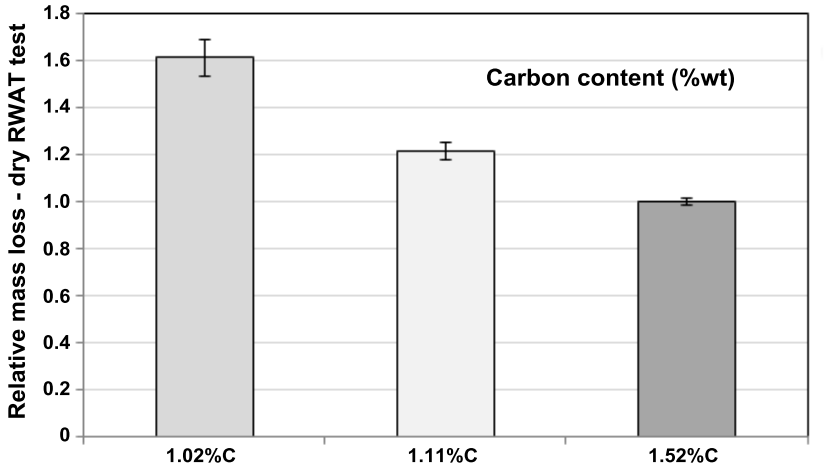

Figure 18. Relationship between the relative mass loss (reference material ASTM H13 steel 514 ± 5 HV) and carbon content of manganese steel, with coarse abrasive particle size. Dry RWAT, silica (+300 – 600 µm, 130 N, 10 min) [13].

The decrease in mass loss with increasing carbon content was confirmed by dry and wet rubber wheel abrasion tests, performed on the alloys with the largest differences of carbon content; results shown in Figure 19.

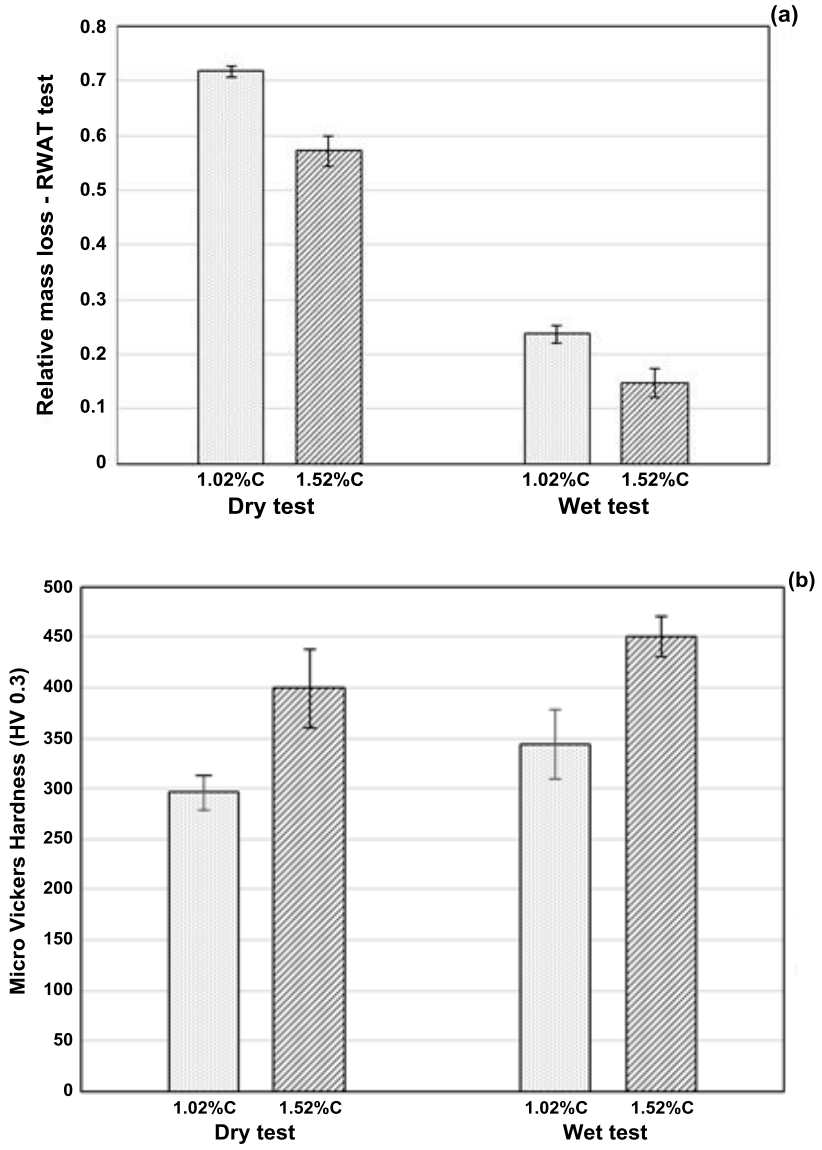

Figure 19. Relationship between the relative mass loss (reference material ASTM H13 steel 514 ± 5 HV) and carbon content of manganese steel, with fine abrasive particle size. Dry RWAT, silica (–300 + 150 μm, 130 N, 10 min) [13].

The effect of increasing carbon content was the same for both dry and wet tests, as was observed with the large abrasive grain size (600 -v- 150 μm) in Figure 18. After dry and wet abrasion tests, measurements showed that surface hardness was higher for the high carbon steel. Therefore, it is hypothesized that the higher carbon content has promoted a more intense work hardening for the high carbon alloy than for the low carbon one and that resulted in lower mass loss of the high carbon alloy in the three test conditions.

The paper of Diesburgh and Borik [14], presents supportive information about such findings regarding the abrasion resistance of manganese steels. The authors performed a series of jaw crusher tests on nine Hadfield steels for which chemical compositions, hardness and wear results are displayed in Tables VI and VII where the gouging wear ratio is the ratio between the mass losses of a sample and the mass loss of a reference material.

Table VI. Chemical Composition of Hadfield Steels, wt.%

Code No.	Materials	Element, %								
		C	Mn	Si	Cr	Ni	Mo	P	S	Other
40	12Mn-1Mo	0.65	12.74	0.51	-	-	0.96	-	-	
41	12Mn	0.93	12.97	0.5	-	-	-	-	-	
42	12Mn-1Mo	0.93	12.0	0.5	-	-	1.0	-	-	
43	12Mn-1Mo	1.09	12.5	0.5	-	-	0.94	-	-	
44	12Mn	1.10	12.5	0.5	-	-	-	-	-	
45	12Mn	1.24	12.5	0.5	-	-	0.05	-	-	
46	12Mn-1Mo-Ti	1.26	12.5	0.5	-	-	0.96	-	-	0.25Ti
47	12Mn-1Mo-Ti	1.29	12.5	0.5	-	-	0.94	-	-	0.18Ti
48	12Mn-1Mo-Ti	1.29	12.5	0.5	-	-	1.02	-	-	0.13Ti
49	12Mn-1Mo-Ti	1.31	12.5	0.5	-	-	0.92	-	-	

- Not analyzed

Table VII. Hardness, Wear Results and Impact Energy of Hadfield Steels

Code No.	Type of Steel	HB	Charpy V-notch Energy (ft-lb)	Charpy V-notch Energy (J)	Gouging Wear Ratio	Weight Loss (g)	Principal Components of Microstructure *
						Pin	
40	12Mn-1Mo (0.65C)	191	88	119	0.42	-	A
41	12Mn (0.95C)	185	102	138	0.33	0.0871	A
42	12Mn-1Mo (0.95C)	188	53	72	0.32	-	A,P
43	12Mn-1Mo (1.09C)	192	107	145	0.29	0.0821	A
44	12Mn (1.1C)	199	-	-	0.28	-	A
45	12Mn (1.25C)	198	59	80	0.21	-	A
46	12Mn-1Mo-Ti (1.25C)	201	53	72	0.21	-	A
47	12Mn-1Mo-Ti (1.3C)	204	64	87	0.22	-	A
48	12Mn-1Mo-Ti (1.3C)	201	57	77	0.22	-	A
49	12Mn-1Mo-Ti (1.3C)	199	25	34	0.21	-	A

* A - austenite, P - pearlite

The relative mass loss data from the jaw crusher tests from Table VII are plotted in Figure 20 [14]. The decrease of abrasion losses with increasing carbon content, foreseen in the limited results from Figures 18 and 19, was confirmed with this larger number of experiments and in a quite distinct tribosystem, more related to the application where those alloys are used.

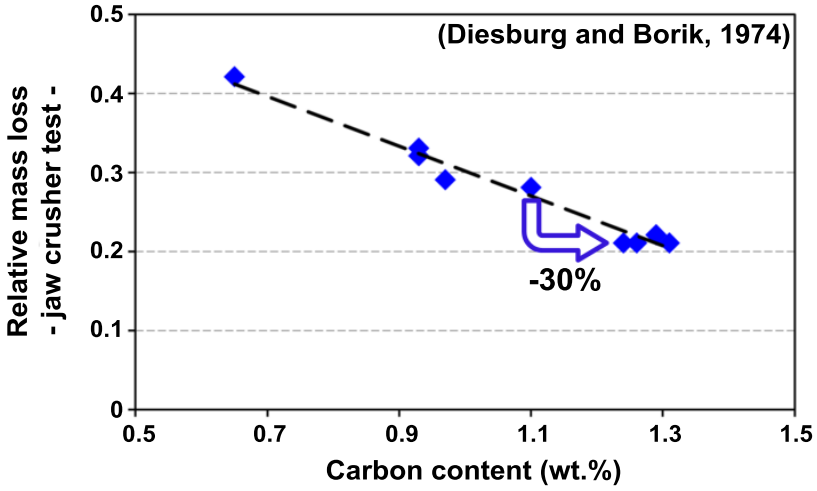

Figure 20. Relationship between the relative mass loss and carbon content of manganese steel. Jaw crusher tests [14].

Increasing the (dissolved) carbon content from 1.05 to 1.35%, ie. the bottom and upper limit of the ASTM class "C" manganese steel standard, resulted in a decrease in the relative mass loss from 0.28 to 0.20, approximately 30%. Each 0.1% of carbon resulted in a 10% increase of abrasion resistance. The effect of carbon in Figures 18 and 19 is around 7% per 0.1% carbon. This achievement was not highlighted by the authors at the time of the publication [14].

Environment

The last of the effects, not directly connected to hardness, is the effect of the environment, as presented in Figure 21.

Two distinct tendencies can be seen in Figure 21. As the abrasive particle size increased, the abrasion also increased, at first strongly, as the abrasive grain size increased from 0.15 to 0.60 mm. After that, the increase in abrasion occurred at a lower rate. The second trend is that the abrasion was more intense at lower pH values for all the grain sizes. The decrease in the abrasive wear rate from the lowest to the highest pH lies on the range ~20 to 80% depending on the abrasive particle size, an effect that may be more pronounced than some of the hardness and microstructural effects studied before in this paper. The reason for this behavior is not yet fully understood.

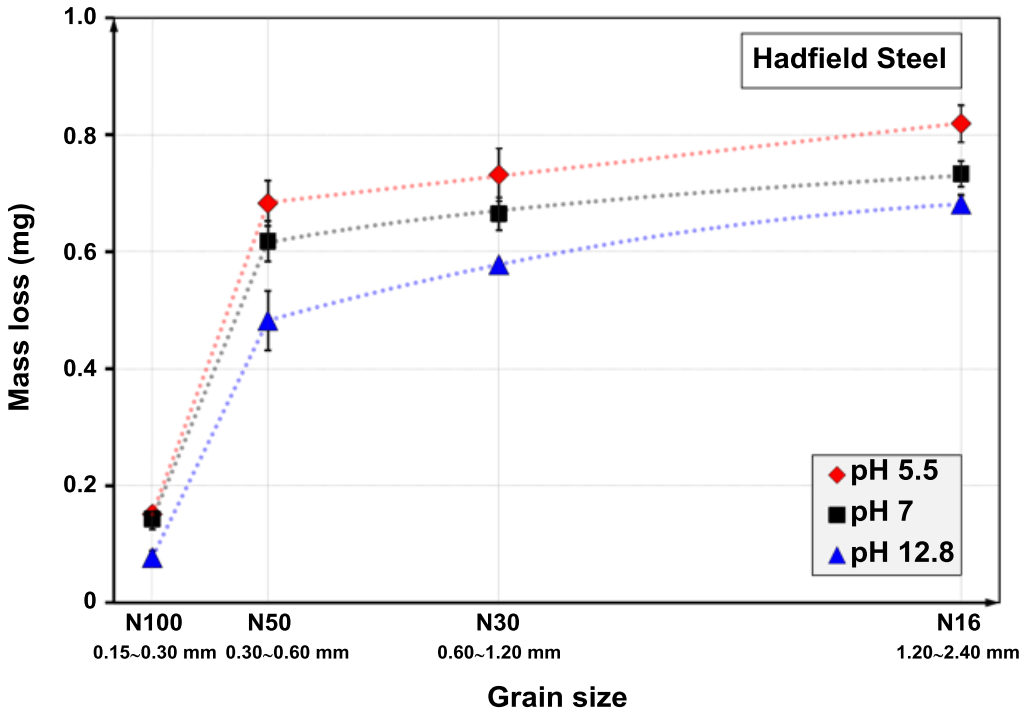

Figure 21. Relationship between abrasive grain size, pH and mass loss of manganese steel. Wet RWAT, (Hadfield composition: 1.11%C, 14.2%Mn and 1.81%Cr). Tressia [15].

Conclusions

The relationship between laboratory tests and field performance is a complex subject still open to discussion and investigation. However, the results show clearly that laboratory wear tests performed under test conditions more severe than those found in field service will underestimate the benefits of improving material hardness. Since this improvement is achieved at higher costs, the benefits can be underestimated as a consequence of severe conditions of the laboratory test.

Relatively small hardness decreases due to casting, welding, and heat treatment variations will strongly reduce the abrasion resistance of the components that are used in the transition region between mild and severe wear. In other words, transferring laboratory results to field operations requires careful follow-up, in order to assure that sound and reliable materials like the ones tested in a laboratory will be applied to each piece of equipment.

Hardness and hard, large phases are key factors to produce high abrasion resistant materials.

Niobium plays a decisive role in increasing abrasion resistance of materials for the mining industry. The shape, size and distribution of niobium carbides need to be engineered to achieve the maximum effect.

Acknowledgements

The authors acknowledge the companies CBMM (Companhia Brasileira de Metalurgia e Mineração), ThyssenKrupp Fördertechnik Latino Americana and Vale for supporting research activities. A special thanks to researchers in the area of abrasion that have been part of the Surface Phenomena Laboratory: Luiz Alberto Franco, Gustavo Tressia de Andrade, Jimmy Penagos, Juan Ignacio Pereira, Paulo Machado, Marcos Henrique Ara, Giuseppe Pintaúde, John Jairo Coronado, Marcio Matos Santos, Felipe Gustavo Bernardes, Sara Aida Rodríguez Pulecio and Leonardo Villabón.

References

1. K. Holmberg, "Reliability Aspects of Tribology," *Tribology International*, 34 (12) (2001), 801–808.

2. E. Rabinowicz, L.A. Dunn and P.G. Russell, "A Study of Abrasive Wear Under Three-body Conditions," *Wear*, 4 (5) (1961), 345-355.

3. J. Gates, "The Challenge of Accurate Prediction of Industrial Wear Performance from Laboratory Tests," Paper presented at the Intenational Symposium on Wear Resistant Alloys for the Mining and Processing Industry, Campinas 2015.

4. J.D. Gates, "Two-body and Three-body Abrasion: A Critical Discussion," *Wear*, 214 (1) (1998), 139-146.

5. K. Zum Gahr, *Microstructure and Wear of Materials* (Amsterdam, The Netherlands: Elsevier Science Publishers B.V., 80-131, 1987.

6. G. Pintaude et al., "Mild and Severe Wear of Steels and Cast Irons in Sliding Abrasion," *Wear*, 267 (1-4) (2009), 19-25.

7. J.J. Coronado, S.A. Rodríguez and A. Sinatora, "Effect of Particle Hardness on Mild-severe Wear Transition of Hard Second Phase Materials," *Wear*, 301 (1-2) (2013), 82-88.

8. A.A. Torrance, "An Explanation of the Hardness Differential Needed for Abrasion," *Wear*, 68 (2) (1981), 263-266.

9. J.J. Penagos, G. Tressia and A. Sinatora, "Abrasive Wear Tests on Materials used for Wear Plates" (Surface Phenomena Laboratory Technical Report TK 03-1-001-Rev0 for ThyssenKrupp Fördertechnik Latino Americana - TKFLA, 2014).

10. J.J. Penagos and A. Sinatora, "The Effect of Structure Refinement and Niobium Addition on Abrasion Resistance of White Cast Irons used for Slurry Pump Impellers" (Surface Phenomena Laboratory Technical Report NB01-2-003-Rev0 for CBMM - Companhia Brasileira de Metalurgia e Mineração, 2013).

11. J.J. Penagos et al., “Structure Refinement Effect on Two and Three-body Abrasion Resistance of High Chromium Cast Irons,” *Wear*, (doi:10.1016/j.wear.2015.03.020) (2015).

12. P.F. Silva and M. Jr. Boccalini, “Abrasive Wear of Nb-alloyed High Speed Steels,” *Proceedings of the First International Brazilian Conference on Tribology*, Rio de Janeiro, Brazil, 26 November 2010.

13. P. Machado and A. Sinatora, “Abrasive Wear Tests on Hadfield Steels Extracted from Field Samples” (Surface Phenomena Laboratory Technical Report VL0X-1-001-Rev0 for VALE, 2015).

14. D.E. Diesburg and F. Borik, *Optimizing Abrasion Resistance and Toughness in Steels and Irons for the Mining Industry*, (Materials for the Mining Industry Vail Co. Climax Molybdenum Co., 1974). 15-42.

15. G. Tressia, “Abrasion Resistance of Hadfield Steel for Crushers–Effect of the Abrasive Grain Size on pH” (Master Degree Dissertation, 2015), 127.